Desalination 404 (2017) 138–146

Contents lists available at ScienceDirect

Desalination

journal homepage: www.elsevier.com/locate/desal

A power free electrodialysis (PFED) for desalination

Fabao Luo [a,b], Yaoming Wang [a], Chenxiao Jiang [a], Bin Wu [a], Hongyan Feng [a], Tongwen Xu [a,*]

[a] Collaborative Innovation Center of Chemistry for Energy Materials, School of Chemistry and Material Science, University of Science and Technology of China, Hefei 230026, PR China
[b] Department of Chemistry and Chemical Engineering, Hefei Normal University, Hefei 230061, PR China

HIGHLIGHTS

- A power free electrodialysis (PFED) for water desalination was explored.
- The PFED can achieve a synergistic enhancement effect on water desalination.
- The PFED realize zero discharge of high salt wastewater.
- The conductivity of fresh water can be as low as 72 μS cm^{-1}.

GRAPHICAL ABSTRACT

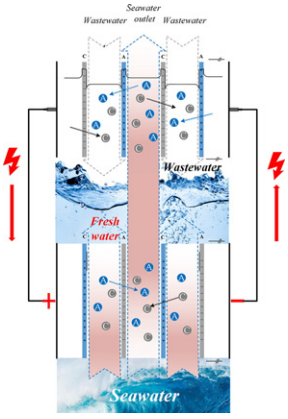

ARTICLE INFO

Article history:
Received 12 August 2016
Received in revised form 8 October 2016
Accepted 7 November 2016
Available online 16 November 2016

Keywords:
Power free
Reverse electrodialysis
Electrodialysis
Desalination
Process integration

ABSTRACT

A power free electrodialysis (PFED) is proposed for water desalination by integrating with a reverse electrodialysis (RED) as an energy donor. The effects of flow rates, salt concentration ratio between high salt concentration compartment (HC) and low salt concentration compartment (LC) on energy generation are investigated. The combination of ED and RED for fresh water production is attempted and the desalination performances in both continuous and batch-wise modes are investigated. The results show that the integration is feasible and the conductivity of the product water can be as low as 72 μS/cm, which is indubitably qualified for drinking. To test the robustness of this hybrid technology, the batch-wise mode is chosen to generate power from simulated seawater and wastewater. It is found that the PFED can be successfully carried with no significant desalination difference compared to NaCl solution. PFED is thus confirmed to be technically feasible, and economically attractive for water desalination without the consumption of external energy.

1. Introduction

The requirement for fresh water is going up substantially due to the increase of human being and industrial growth in many parts of the world [1,2]. Desalination technologies can greatly alleviate water shortage problems [3–6]. Currently, either thermal (phase-change) processes or membrane processes are used for water desalination with a negative impact on the environment due to their intensive energy consumption and concentrated brine disposal [7]. As one of the desalination technologies, Electrodialysis (ED) can produce both freshwater and table salt from salty water with the aids of ion exchange membranes and direct

* Corresponding author.
E-mail address: twxu@ustc.edu.cn (T. Xu).

http://dx.doi.org/10.1016/j.desal.2016.11.011
0011-9164/

Nomenclature

A	effective area of a single membrane (m^2)
a_c	activity of the concentrated salt solution (mol/L)
a_d	activity of the diluted salt solution (mol/L)
AEM	anion exchange membrane
b	compartment width (cm)
C_c	the concentration of HC (mol/L)
C_d	the concentration of LC (mol/L)
C_m	the mix average concentration (mol/L)
CEM	cation exchange membrane
d_c	the thickness of HC (cm)
d_d	the thickness of LC (cm)
E_{OCV}	theoretical open stack circuit potential (V)
E_x	the maximum released energy of mixing the two salt solutions(W)
ED	electrodialysis
F	Faraday constant (96,485 C/mol)
HC	high salt concentration compartment
I	current (A)
LC	low salt concentration compartment
N	number of cell pairs for RED
$N`$	number of repeating units for ED
P	output power (W)
P_{gross}	maximum gross power density (W/m^2)
P_{max}	maximum output power (W)
P_{net}	net power density (W/m^2)
P_{pump}	power density consumed for pumping (W/m^2)
$PFED$	power free electro dialysis
Q	volumetric flow rate (mL/min)
Q_c	volumetric flow rate of HC (L/s)
Q_d	volumetric flow rate of LC (L/s)
R	gas constant (8.314 J/mol/K)
R_a	the resistance of anion exchange membrane (Ω/cm^{-2})
R_{BL}	boundary layer resistance (Ω)
R_c	the resistance of cation exchange membrane (Ω/cm^{-2})
R_{el}	the resistance of electrodes (Ω)
R_{load}	load resistance (Ω)
R_{ohmic}	Ohmic resistance (Ω)
R_{stack}	stack resistance (Ω)
$R_{\Delta C}$	concentration difference resistance (Ω)
RED	reverse electrodialysis
T	absolute temperature (K)
V	line flow velocity (cm/min)
z	electrochemical valence
α	average membrane permselectivity of an anion and a cation exchange membrane pair
δ	spacer thickness (cm)
ε_{sp}	spacer porosity
κ_c	the specific conductivity of the concentrated solution (mS/cm)
κ_d	the specific conductivity of the diluted solution (mS/cm)
Δp_c	the pressure drops along HC (KPa)
$\Delta p_{d.}$	the pressure drops along LC (KPa)

current [8]. Due to the utilization of electricity, the energy consumption accounts for almost half of total process cost, such as energy cost, capital investment, and operational and maintenance cost, etc. [5,7,9]. Besides, in some isolated locations, remote areas, or islands, an electricity supply is not reliable and the water scarcity becomes even more severe [10]. Therefore, some renewable energy such as solar, wind and geothermal energy were used to drive the desalination processes. Due to the expensive equipment and complicated technologies, the production cost of the fresh water by these renewable energy is often much higher than that by the conventional energy. However, considering the shortage of fossil fuel energy, renewable energy is receiving much more attention for water desalination [3,7,11,12].

Reverse electrodialysis (RED) is an emerging renewable energy technology to generate electrical power from two salinity gradient solutions [13–15]. It uses ion-exchange membrane for ion transport based on the concentration difference as driving force. The ionic diffusive flux generates an electrochemical potential recorded as a voltage across electrodes. Electrodes receive the ions and convert into an electrical current with an oxidation or reduction reaction. The generated electrical current can be collected by an external load. Thus, RED process can harvest clean energy from the ambient environment in an economically competitive manner. The pioneering work in the field of RED was proven by Pattle [16], who used an apparatus called hydroelectric pile to generate electric power. In order to improve the power density, the ion exchange membrane formation and membrane stack structure designs were the hotspots of RED researches [17–20]. Recently, a membrane stack was designed with two parts of RED and ED for energy self-sufficient desalination. This self-desalination process is appropriate for changing the brine water into fresh water on small islands [21]. However, there are limited reports on the in-situ combination of RED and ED for water desalination, except for some integration process supplying the high salt water for RED [22–24]. These few reported self-desalination with ED and RED in the same stack usually has a poor desalination performance and a synergistic intensification of two processes is not achieved.

Herein, a power free electrodialysis (PFED) is designed by an in-situ combination of ED and RED unit. RED is used as the energy donor and ED is used as the energy acceptor. As a consequence, this hybrid process can abandon the use of cumbersome batteries or external power supplies as well as the disposal of concentrated brines. A full-scale RED module is very similar to that of conventional ED, which is consisted of high salt concentration compartment (HC), low salt concentration compartment (LC), ion-exchange membranes and electrode rinse solutions. This process intensification of ED and RED can achieve a synergistic enhancement effect on water desalination. On one hand, the concentrated brine output from ED can be fed into HC of RED, thus further enhancing the power output; on the other hand, LC of RED in the integrated system can be supplied even from the life wastewater, so freshwater can be obtained in an economically competitive manner.

2. Theory and experiment

2.1. Theory

The theoretical value of the potential over an ion exchange membrane for an aqueous monovalent ion solution (e.g. NaCl) can be calculated using the Nernst equation in Eq. (1) [25–27]:

$$E_{OCV} = N\frac{2\alpha RT}{zF}\ln\left(\frac{a_c}{a_d}\right) \tag{1}$$

where E_{OCV} is the theoretical open stack circuit potential (V), α is the average membrane permselectivity of an anion and a cation exchange membrane pair, N is the number of cell pairs, R is the gas constant (8.314 J/mol/K), T is the absolute temperature (K), z is the electrochemical valence, F is the Faraday constant (96,485 C/mol), a_c is the activity of the concentrated salt solution (mol/L) and a_d is the activity of the diluted salt solution (mol/L). The power produced is related to the electrochemical potential drop across the membrane, E_{OCV}, and an external load resistance resulting in Eq. (2) [25,28]:

$$P = I^2R_{load} = \frac{{E_{OCV}}^2}{(R_{stack}+R_{load})^2}R_{load} \tag{2}$$

In this equation, P is the output power (W); I is the current (A); R_{load} and R_{stack} are the resistances of the load and stack resistance (Ω), respectively.

The maximum power output of the system is obtained when R_{load} equals to the resistance of the stack (R_{stack}) [25]. Thus, the maximum output power can be simplified into Eq. (3),

$$P_{max} = \frac{{E_{OCV}}^2}{4R_{stack}} \tag{3}$$

Consequently, the power density (power output per unit membrane area, P_{gross}) can be calculated from P_{max} [25], as shown in Eq. (4).

$$P_{gross} = \frac{P_{max}}{2AN} = \frac{{E_{OCV}}^2}{8ANR_{stack}} \tag{4}$$

where P_{gross} is the maximum gross power density (W/m^2), P_{max} is maximum output power (W), A is effective area of a single membrane (m^2). The presence of spacers will significantly decrease the power output due to the loss of the membrane area from non-conductive spacer blockage.

The total resistance of an RED stack includes those of electrodes, electrolytes, diffusion boundary layers at the membrane surface, and membranes. Simplified models neglect the resistance of diffusion boundary layers or combine its contribution with membrane resistance and express the overall resistance(Ω) as Eq. (5) [15,19,26],

$$R_{stack} = \frac{N}{A}\left(R_a + R_c + \frac{d_c}{\kappa_c} + \frac{d_d}{\kappa_d}\right) + R_{el} \tag{5}$$

where A is the effective membrane area (cm^2); R_a is the resistance (Ω/cm^{-2}) of anion exchange membrane (AEM); R_c is the resistance (Ω/cm^{-2}) of cation exchange membrane (CEM); R_{el} is the resistance (Ω) of electrodes; d_c is the thickness (cm) of HC; d_d is the thickness of LC; κ_c is the specific conductivity (mS/cm) of the concentrated solution; and κ_d is the specific conductivity (mS/cm) of the diluted solution.

Then, due to the concentration change of the different flow paths of a cell after ion migration, the resistances of all the different positions are multipliable with the exception of the electrodes [29]. The electrode resistance may be considered negligible if the stack cells are scaled larger than 20 but with only two electrodes [19]. Considering the effect of the salinity gradient and the diffusion boundary layer resistance, the entire RED stack resistance can be expressed as Eq. (6) [30,31],

$$R_{stack} = \frac{N}{A}(R_{ohmic} + R_{\Delta C} + R_{BL}) \tag{6}$$

where R_{ohmic} is the membrane resistance ascribed to the ionic transport through the membranes, which is equal to the one cell resistance discussed above. $R\Delta_C$ is the resistance ascribed to the reduced electromotive forces as a consequence of the change in the concentration of the bulk solution. It considers the change of the solution concentration from the inlet to the outlet of the solution compartment with the spatial difference of membrane potential. R_{BL} is the boundary layer resistance due to concentration polarization which induced by diffusive boundary layer near the membranes at lower flow rates. Both $R\Delta_C$ and R_{BL} are belonged the significant non-ohmic resistance.

The net power density (P_{net}, in W/m^2) that is generated by a RED stack can be calculated as the difference between the gross power density and the power density consumed for pumping (P_{pump}, in W/m^2) of both feed waters, which can be calculated from the pressure drop over the inlet and outlet and the flow rate per cell areas. Thus, the net power density can be expression as Eq. (7) [22],

$$P_{net} = P_{gross} - P_{pump} = \frac{{E_{OCV}}^2}{8ANR_{stack}} - \frac{\Delta p_c Q_c + \Delta p_d Q_d}{NA} \tag{7}$$

where Δp_c and Δp_d are the pressure drops along HC and LC, respectively. Q_c and Q_d are the volumetric flow rates of HC and LC, respectively.

The maximum released energy (E_x) of mixing the two salt solutions is given by Eq. (8) [32],

$$E_x = 2RT\left[Q_c C_c \ln\frac{C_c}{C_m} + Q_d C_d \ln\frac{C_d}{C_m}\right] \tag{8}$$

where C_c and C_d are the concentration of HC and LC, respectively. The mix average concentration C_m is given by Eq. (9),

$$C_m = \frac{Q_c C_c + Q_d C_d}{Q_c + Q_d} \tag{9}$$

2.2. Experiment section

2.2.1. Experiment operation

The experiments were performed in three steps. At first, the RED process was optimized to obtain the optimum experimental conditions for power generation. Furthermore, a power free electrodialysis (PFED) was attempted to test the feasibility of this integrated process for water desalination by using NaCl solution as the feed solution. Finally, the integrated process was investigated with simulated sea water and wastewater to test the robustness of this integration in a complicated water system.

2.2.2. Experiment setup

A lab-scale RED setup was designed and installed in our lab. A schematic diagram of the RED principle was illustrated in Fig. 1a. The RED setup was composed of (1) a cathode and an anode, which was made of titanium coated with ruthenium and iridium; (2) different cell pairs ($N = 10$ for separated and 20 for integrated operation) of specially prepared cation and anion exchange membranes which were alternatively arranged; and (3) spacers with thickness of 0.75 mm to separate the anion and cation exchange membranes. The RED membranes were specially prepared with a thickness of approximately 50 μm while the ED membranes were kindly provided from Hefei ChemJoy Polymers Co., Ltd., China. The main properties of RED membranes were the same as those for ED process except for the membrane thickness and listed in Table 1. The cell pairs were ten and twenty for RED optimization process and PFED process, respectively. The effective area of each membrane was 189 cm^2. In the RED optimization, three flow streams, i.e. electrode compartment, high salt concentration compartment (HC), low salt concentration compartment (LC) were established. A 500 mL electrode rinse solution was circulated with a peristaltic pump (BT600L, Lead fluid, China) at a flow rate of 75 mL/min. The same flow rate was maintained in HC and LC with two peristaltic pumps (BT600L, Lead fluid, China). The flow stream was "feed-and-bleed" pass through the HC and LC with different velocity (0–700 mL/min).

The ED stack in the PFED process was equipped with the same kinds of electrodes and spacers as the RED stack but with different repeating unit ($N' = 1$, 2, and 4) of ordinary ion exchange membranes (CJ-MA-2 and CJ-MC-2). A schematic diagram of the PFED process is illustrated in Fig. 1b. Three kinds of repeating unit ($N' = 1$, 2, and 4) were compared in ED stack. The pair number of RED stack is twenty in PFED stack. In the PFED process, five flow streams were established. They were ED electrode compartment, low salt concentration compartment (LC) in ED stack, high salt concentration compartment (HC) in ED stack, RED electrode compartment, low salt concentration compartment (LC) in RED stack. It should be noted that the flow stream of HC in ED stack was directly fed into HC in RED to obtain process intensification. The ED and RED electrode compartments were respectively circulated with a peristaltic pump at a flow rate of 75 mL/min.

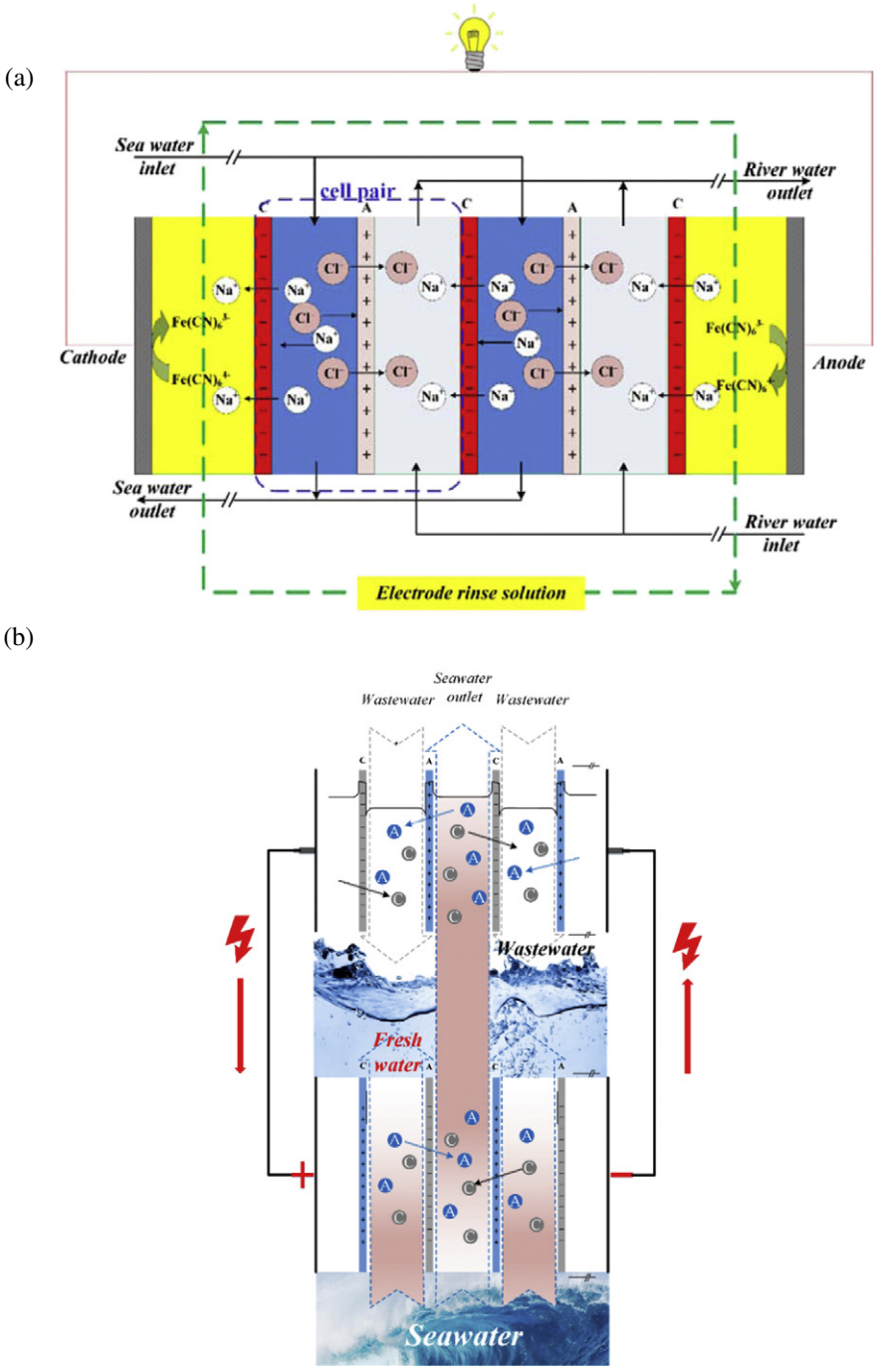

Fig. 1. A schematic diagram of the principle of (a) reverse electrodialysis, RED and (b) power free electrodialysis, PFED.

2.2.3. Feed solution

To optimize the experiment conditions in RED process, the low salt concentration compartment (LC) was fed with solutions containing 1 g/L (or 3 g/L) NaCl; the high salt concentration compartment (HC) was fed with different concentrations (10 g/L, 30 g/L, 70 g/L, and 150 g/L) of NaCl aqueous solution. The electrode rinse solution in RED stack was consisted of 0.05 M $K_3[Fe(CN)_6]$, 0.05 M $K_4[Fe(CN)_6]\cdot 3H_2O$ and 0.25 M NaCl aqueous solution, which was circulated in the electrode compartment at a flow rate of 75 mL/min.

In the PFED process, different amounts of sodium chloride were dissolved in deionized water to obtain different levels of conductivities (2000 μS/cm, 5000 μS/cm and 9000 μS/cm) as the feed of ED stack, respectively. The electrode rinse solution in ED stack is consisted of 0.05 M $K_3[Fe(CN)_6]$, 0.05 M $K_4[Fe(CN)_6]\cdot 3H_2O$ and 0.25 M Na_2SO_4 aqueous solution, which was circulated at a flow rate of 75 mL/min. The desalination performance was monitored by a conductivity meter (DDS

Table 1
The main characteristics of the membranes used in the experiments.

Properties	CJ-MC-2	CJ-MA-2
Thickness, mm	0.200	0.145
Ion exchange capacity, mmol/g	1.50	1.25
Water uptake, %	35	32
Resistance, Ω/cm^2	1.5	1.2
Transfer number, %	98	99
Break stress, MPa	>3.5	>3.5

307 Conductivity Instruments, Leici Instrument, Shanghai, China). To test the robustness of PFED in a complicated water system, simulated seawater and wastewater instead of NaCl were used as feed solutions. As shown in Fig. 1b, seawater was desalinated with ED part for fresh water, which was driven by RED part from the concentration difference of concentrated seawater and waste water. Simulated sea water was prepared by dissolving 30gseacrystal (Qianjiang Sea Crystal Factory, Weifang, China) in 1 L deionized water while the wastewater was prepared by dissolving 0.8 g sodium chloride, 0.1 g potassium dihydrogen phosphate, 0.1 g ammonia chloride, 0.5 g glucose dissolved in 1 L deionized water. All the reagents used were analytical grade and provided by Sinopharm Chemical Reagent Co., Ltd.

3. Results and discussion

3.1. Optimum of RED

To run up the PFED process with RED as an energy donor, the operating parameters of RED should be optimized at first. This section focuses on investigation the effects of flow rate and salt concentration difference between LC and HC on energy generation.

3.1.1. Influence of flow rate

The line flow velocity (V) can be defined as the mean fluid velocity inside a single spacer-filled channel. It can be estimated by Eq. (10) [33],

$$V = \frac{Q}{N \cdot \delta \cdot b \cdot \varepsilon_{sp}} \tag{10}$$

where Q is the volumetric flow rate (mL/min) in HC or LC inlet, δ is the spacer thickness(0.075 cm), b is the compartment width (9 cm for the small stack) and ε_{sp} is the spacer porosity (75% for the woven spacer used in this study). For simplicity, the flow rate in the experiment is expressed as the volumetric flow rate.

Flow rate is one crucial parameter affecting the RED performance, which can be indicated from the internal resistance (R_{stack}), open circuit voltage (E_{OCV}), and power density (P_{gross}) [29]. To investigate the effect of flow rate on energy generation, the flow rate ratio of HC and LC was kept at 1:1. The pair number of membranes in this separated RED stack is ten. Fig. 2a shows the effects of flow rate on internal resistances of the RED stack. It can be seen that the resistance initially increases rapidly, but then reaches a plateau and thereafter remains relatively constant. At low flow rates (Q < 40 mL/min), the residual time of flow stream in the stack is reduced with an increase of the flow rate. In this case, the internal resistance is mainly dependent upon the resistance in LC according to Eq. (5). As a consequence, there is an increasing trend of resistance with an increase of flow rate. At middle flow rates (40 mL/min < Q < 170 mL/min), the resistance in LC almost approaches stable and is not significantly affected by the flow rate. The internal resistance is more likely to be determined by the resistance ascribed to the reduced electromotive forces ($R_{\Delta C}$) and the boundary layer resistance (R_{BL}) as described in Eq. (6). At high flow rates (Q > 170 mL/min), the boundary layer of the RED stack keeps at a very small constant value. Both the resistance ascribed to the reduced electromotive forces ($R_{\Delta C}$) and the boundary layer resistance (R_{BL}) can be neglected. A constant resistance is obtained in this case. Fig. 2b indicates the effects of flow rate on open circuit voltage. The open circuit voltage increases at first and then approaches a constant voltage of 1.4 V. According to Nernst equation in Eq. (1), the open circuit voltage is highly related to the activities in the concentrated and diluted salt solution. The boundary layer is relatively laminar at low flow rates (Q < 40 mL/min) which decreases with an increase in flow rate. Meanwhile, the activity difference between concentrated and diluted salt solution is increased with an increase of flow rate. Therefore, a sharply increase of open circuit voltage is observed in low flow rate range. At middle flow rates (40 mL/min < Q < 170 mL/min), the open circuit voltage increases slowly due to deceleration of boundary layer and the increment of the activities in concentrated and diluted salt solution. At high flow rates (Q > 170 mL/min), both the boundary layers thicknesses and activities in concentrated and diluted salt solution will settle to a steady state. A constant voltage will be maintained in this case. Fig. 2c indicates the dependence of power density on the flow rate. The powder density is related to both the internal resistance and open circuit voltage. It is found that the power density increases at first and then becomes stationary, and it reaches the maximum when the flow rate is 67.5 mL/min (~0.22 cm/s line flow velocity). The output power density is significantly affected by the activities in the concentrated and diluted salt solution as well as the thickness of the boundary layer, and these influences are more pronounced at low flow rate range. By considering the internal resistance and open circuit voltage as well as the power density, the flow rate in the range of 45-180 mL/min is a suitable choice for the RED stack. The flow rate in the further experiment is chosen in this range.

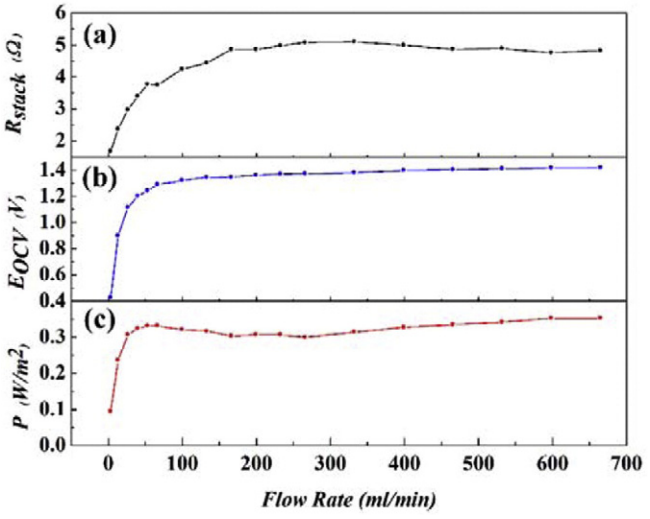

Fig. 2. Influence of flow rate on RED performance. (a) Open circuit voltage, (b)internal resistance, (c) power density. Other experimental conditions: HC, 30 g/L NaCl solution; LC, 1 g/L NaCl solution

3.1.2. Influences of the salt concentration difference between LC and HC

The electricity generated by RED is caused by the diffusion of salt ions from HC into LC. Therefore, the salt concentration in HC and LC has significant influences on energy generation. Fig. 3a and Fig. 3b demonstrate the effects of salt concentration difference between LC and HC on open circuit voltage and the power density of RED stack under different flow rate. It should be noted that the number in the legends of Fig. 3 denotes the weight concentration of salts. For example, LC-HC (1 − 30) means the NaCl concentrations in LC and HC are 1 g/L and 30 g/L, respectively. It is interesting to find that with an increase in the flow rate, the open circuit voltage increases more apparently at higher salt concentration difference. This is due to the change in activities of both concentrated and diluted salt solution, which is more noticeable at the high flow rate and high salt concentration. The similar explanation can be applied for the power density. It is also interesting to find that the open circuit voltages increase at first when the ratio is <30 but then decrease when the ratio is larger than 70. The open circuit voltages at LC-HC (1–150) are even lower than that at LC-HC (1–30) or LC-HC (1–70). This phenomenon may be attributed to the following reasons. One is the concentration polarization [20]. The salt concentration in the boundary layer of LC will be relatively high when a very high salt concentration is applied in HC. Therefore, the activity ratio between HC and LC at an extremely high salt concentration will be lower than that at a moderate salt concentration. Another one is that the permselectivities of ion exchange membranes are decreased at the case of a high concentration [34]. Meanwhile, different open circuit voltages were obtained for the same

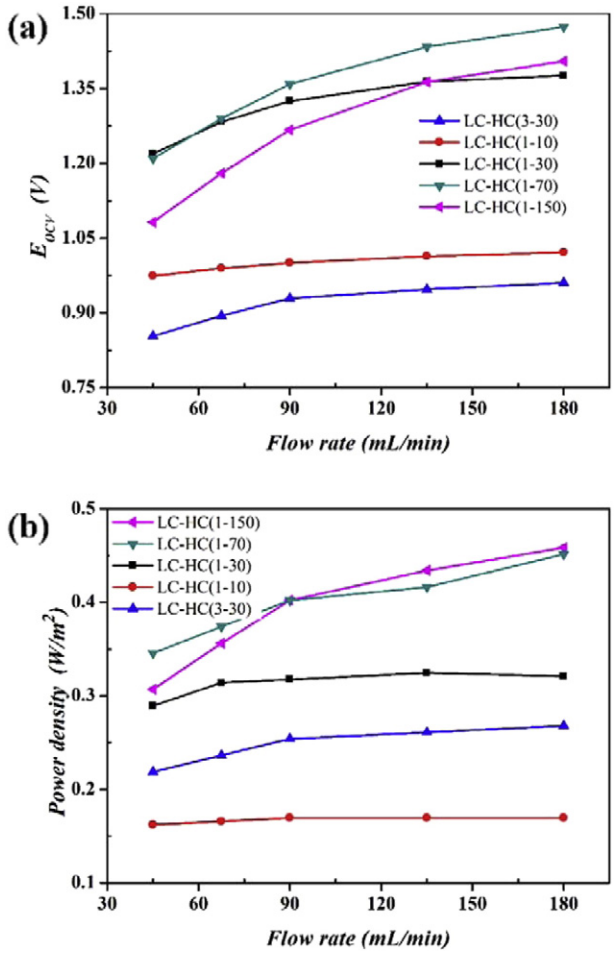

Fig. 3. Influence of the concentration ratio of high concentration compartment (HC) and low concentration compartment (LC) on RED performance under different flow rate. (a) Open circuit voltage, (b) power density. Note. The number in the legends denotes the weight concentration of NaCl. For example, LC-HC (1–30) means the NaCl concentrations in LC and HC are 1 g/L and 30 g/L, respectively.

concentration ratio but at different concentration, such as LC-HC (1 — 10) and LC-HC (3 — 30). A lower open circuit voltage for the same concentration ratio but higher salt concentration is also attributed to the concentration polarization and the permselectivities decrement of the ion exchange membranes. When it comes to the power density, it is found that the power densities increase at first when the concentration ratio is smaller than 70 and thereafter keep almost constant. The conductivities in both HC and LC are increased with an increase in concentration. But open circuit voltages are not further increased when the concentration ratio is larger than 70 as aforementioned. As a result, the highest power density is obtained for the LC-HC (1–70). Meanwhile, the power densities for LC-HC (1–10) are about 30% lower than that for LC-HC (3–30). This indicates the internal resistance rather than open circuit voltage is the most prominent factor affecting the power generation. In addition, the energy generation in Eq. (8) has indicated that the maximum energy output is mainly determined by flow rate and concentration in the HC. A high concentration in HC is beneficial for the maximum energy release. But a high power density is required to maintain a high energy utilized efficiency by considering the energy consumption for pumping according to Eq. (7). Our experiment indicates that LC-HC (1–30) has a relatively high power density and high energy utilized efficiency as well as the highest open circuit voltage. It is conformed to the literature [34]. Therefore, the RED stack with LC-HC (1–30) at the flow rate of 67.5 mL/min is chosen for the further integration experiments.

3.2. Integrating RED and ED with NaCl solution

A power free electrodialysis (PFED) stack was assembled by a combination of RED with ED. To test the feasibility of this integration, aqueous sodium chloride solutions were applied as the feed solutions at first. RED and ED are acted as a pair of energy's donor and acceptor, respectively. This integration in a closed loop circulation offers several benefits. At first, it is no energy except pumping will be consumed. The power consumption for ED comes from two gradient salinity waters in RED. Furthermore, process intensification can be achieved in this combined process. The concentrated brine from ED can be delivered to the HC in RED, thus enhancing the power output. The increase of energy generation in RED can further improve the desalination performance in ED process. Moreover, it is possible to generate fresh water from brine by avoiding the directly discharge of the high salinity wastewater. Because the driven force of ED is generated by the concentration-gradient in RED, this combined stack can work up when the membrane area of ED is much less than that of RED. Therefore, the effect of repeating unit of membrane in ED on the integrated performance was investigated when the RED cell pair number is fixed at twenty. Two operational modes in ED were considered. One is continuous mode where the flow stream is “feed-and-bleed” pass through the ED stack. The other is batch-wise mode where the flow stream is circulated in ED stack with a circulation pump. Fig. 4 illustrates a schematic diagram of these two operation modes.

Fig. 5 indicates the desalination performance of integrated stack in a continuous mode under different LC flow rates in ED stack. It should be noted that the optimum flow rate in RED stack is 67.5 mL/min for a ten pair of membranes as aforementioned. The flow rates in RED stack in this integrated stack are fixed at 135 mL/min for a twenty pair of membranes. As shown in Fig. 5a, all the conductivities are decreased from the initial feed conductivity of 2000 μS/cm, indicating the successful accomplishment of the power free electrodialysis. The conductivities in the desalinated water after the experiments are almost increased with the increase of the LC flow rate except for the four repeating unit ED stack. Because the salts and their concentrations in the HC and LC of RED are fixed, the voltage generated by RED is thus constant. The resistance in the ED stack is folded increase with an increase in the repeating unit of the membranes. In fact, the RED can be considered as a constant voltage “battery” while the ED can be considered as a “load” resistance. During the experiment, the resistances in the ED stack are always increased due to the desalination of salt ions. Different desalination performances are obtained for different repeating unit of ED stack. For one repeating unit ED stack ($N' = 1$), the ED stack resistance is much less than the RED internal resistance. This is shown in Fig. 5b since the ED voltage is only 0.3 V for one repeating unit ED stack. As indicated in Eq. (3), the maximum power output of the system is obtained when the loading resistance equals to RED stack resistance. In other words, the power output is low when the loading resistance is much higher or less than the RED stack resistance. Therefore, a poor desalination performance is obtained for one repeating unit ED stack. For two repeating unit ED stack ($N' = 2$), the ED stack resistance is very close to RED internal resistance. The ED resistance almost equals to RED internal resistance when the flow rate in LC of ED stack is 10 mL/min. The best desalination performance is observed in this case with the lowest conductivity at 736 μS/cm in the desalinated water. For four repeating unit ED stack ($N' = 4$), ED resistance is a slightly higher than RED internal resistance. In this case, the ED resistance with four repeating units is not double compared with that of two repeating units by considering a relative constant resistance in the electrode chambers. An increase in membrane area will not lead to an improved desalination performance due to a decrement in current in this case. Therefore, the desalination performance in four-repeating unit ED stack is very similar to that of two-repeating unit stack. It is interesting to find that desalination performance for four-repeating unit ED stack is even worse than that for two-repeating unit ED stack when the flow rate of LC is 10 mL/min. This is due to a relatively laminar boundary

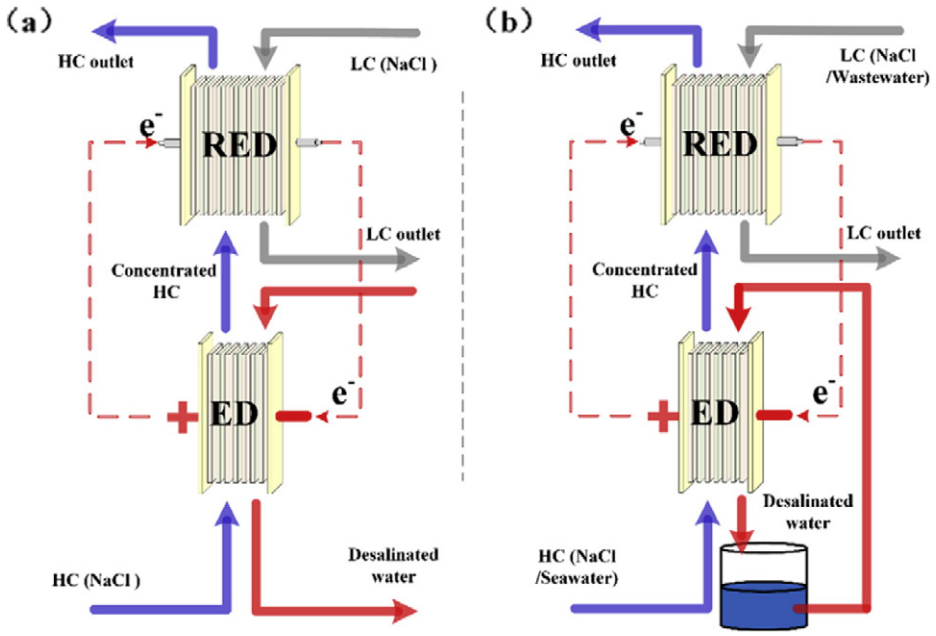

Fig. 4. Schematic diagrams of two operational modes in integrated ED and RED process. (a) Continuous mode; (b) batch-wise mode.

layer in LC of ED stack at such low flow rate. The voltages in ED stack with different repeating units are shown in Fig. 5b. The more the repeating units are, the higher the voltage will be, because the loading resistance increases with the repeating units. However, with an increase in flow rate of LC, the resistance is decreased until a plateau value is reached for each case.

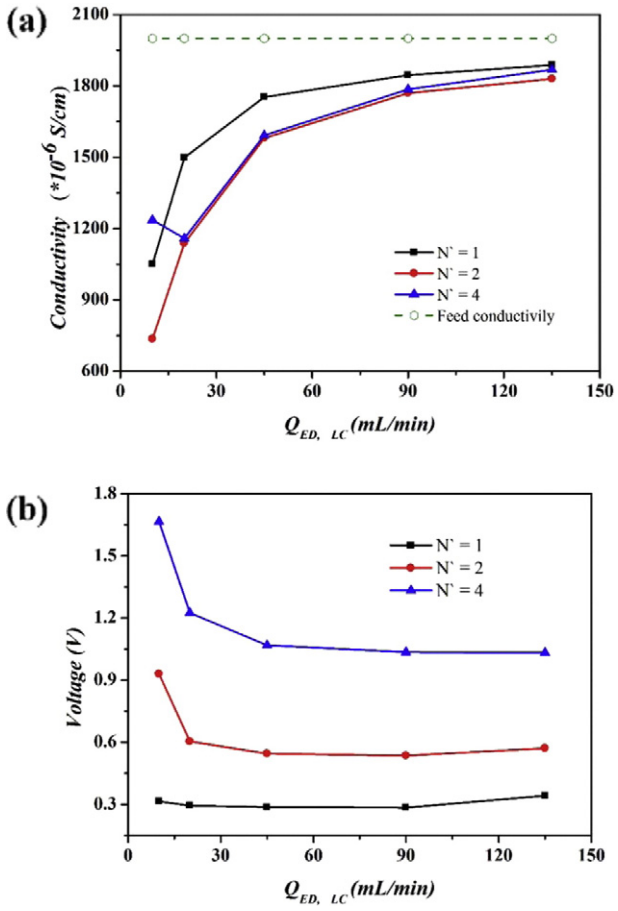

Fig. 5. Desalination performance of integrated ED and RED in a continuous mode. (a) Conductivity of the desalinated water; (b) the voltage of ED. Other experimental conditions: RED pair number is 20; flow rate in the other compartments are 135 ml/min. Note. The number in the legend denotes the repeating unit in ED stack.

Due to the small membrane area of the experimental stack, the continuous mode with "feed-and-bleed" pass through of flow stream has relatively high conductivity in the desalted water. To investigate the desalination performance of the power free electrodialysis with a much higher salinity solution, a batch-wise mode was investigated with a conductivity of 9000 μS/cm chloride sodium solution as feed solution. Fig. 6 indicates the desalination performance of integrated stack in a batch-wise mode for two- and four-repeating unit of ED stacks, respectively. As shown in Fig. 6a, the conductivity in the feed solution is decreased with the elapse of time at each case. Finally, conductivity of the desalinated water decreased to ~72 μS/cm from the initial 9000 μS/cm, indicating the high desalination capacity. But the desalination capacity is not proportional to the repeating unit in the ED stack, as confirmed by the fact that the experiment period with four-repeating unit ED stack is not half of that with two-repeating unit ED stack. Because the ED stack occupies only a fractional part of the PFED stack. This can be indicated by the voltages in the ED stack, as shown in Fig. 6b. It is noted that the voltages in the ED stack increase slowly at first but then rapidly. In the initial period of experiment, the ED stack resistance is lower than RED resistance. However, the ED resistance continuously increases with the PFED experiment. In the later period of experiment, the ED stack resistance will overwhelm the RED stack. In this case, the ED stack resistance will become the dominant contribution to the integrated stack resistance. This result illustrates that only increase the repeating unit in ED stack is not sufficient for an improved desalination performance in the PFED process. It is suggested that a high-effective PFED should be operated when ED stack resistance is equal to RED resistance.

3.3. Integrating RED and ED with simulated sea water and wastewater

The concept of PFED is successfully verified in the above section. To test the robustness of this integration at a complicate feed solution, integrated RED and ED with simulated sea water and wastewater was also investigated. The integrated experiment was performed in a batch-wise mode with four-repeating unit ED stack. Fig. 7 indicates the desalination performance of PFED with simulated sea water and

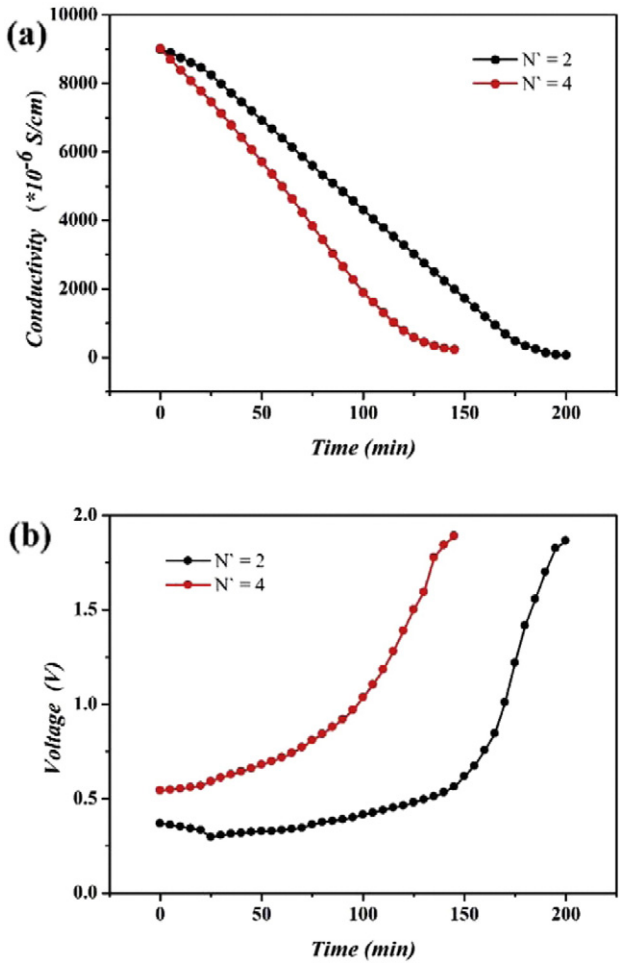

Fig. 6. Desalination performance of integrated ED and RED in a batch-wise mode. (a) Conductivity of the desalinated water; (b) the voltage of ED. Other experimental conditions: RED cell pair number is 20; flow rate in the other compartments are 135 mL/min; the volume of desalinated water is 250 mL. Note. The number in the legend denotes the repeating unit of membrane in ED stack.

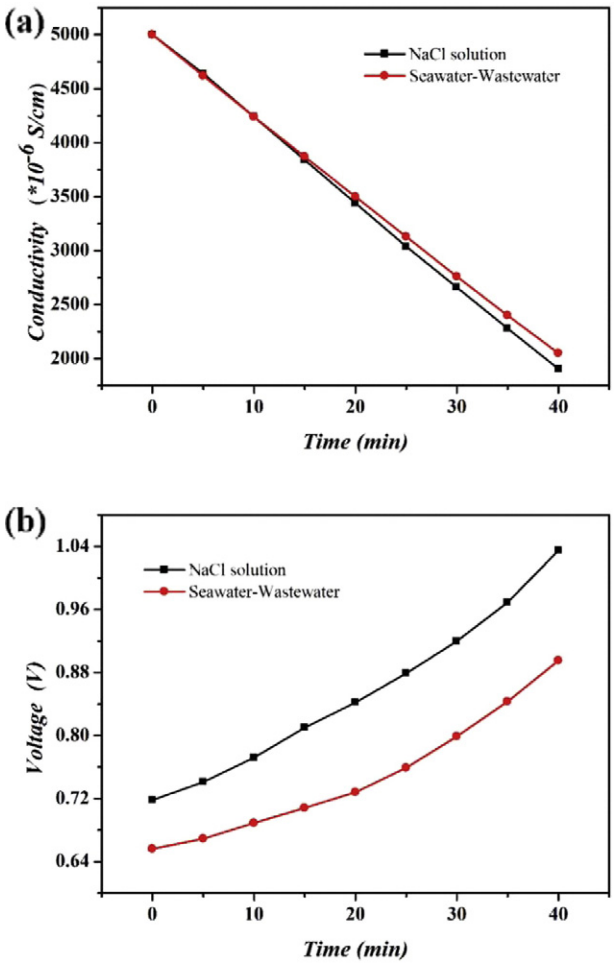

Fig. 7. Desalination performance of integrated ED and RED with simulated sea water and wastewater in a batch-wise mode. (a) Conductivity of the desalinated water; (b) the voltage of ED. Other experimental conditions: RED cell pair number is 20; ED repeat unit number is 4; Flow rate in the other compartments are 135 mL/min; the volume of desalinated water is 250 mL.

wastewater. The desalination performance was compared with the above NaCl solution as the feed solution. As shown in Fig. 7a, the conductivity curve of simulated sea water and wastewater is almost the same as the NaCl solution. This is due to the same concentration rate between LC and HC of RED in both NaCl solution and simulated water. At the same time, Fig. 7b shows the voltage in ED with NaCl solution is even higher than that with simulated water. At the two cases, the concentration gradients can be considered to be identical, which allow the same total voltage by RED. This total voltage will be distributed between the RED and ED units according the respective internal resistance. Compared with pure NaCl solution, the simulated solution will cause an increase in internal resistance of RED and thus voltage in ED at this case is relatively decreased. Nevertheless, it is feasible to produce fresh water by integrated ED and RED with sea water and wastewater.

4. Conclusion

A power free electrodialysis (PFED) was proposed with reverse electrodialysis (RED) as an engine for electrodialysis (ED). Firstly, the RED process was optimized from both the flow rate and concentration difference between LC and HC. The results indicated the NaCl concentrations in LC and HC are 1 g/L and 30 g/L with the flow rate of 67.5 ml/min (0.22 cm/s line flow velocity) were the optimum conditions for RED experiment. Secondly, an in-situ integration of ED with RED was operated at both a continuous mode and a batch-wise mode. Desalted water with ~72 μS/cm conductivity was obtained in a batch-wise mode. Thirdly, the combined process is also successfully carried out with simulated sea water and wastewater. The highest power output for PFED occurs at the case where internal resistances of RED and ED units are equal. In conclusion, it is technically feasible, and economically attractive to produce fresh water from two concentration gradient water without the consumption of external energy.

Acknowledgements

This project has been supported by the National Natural Science Foundation of China (No. 21490581), National High Technology Research and Development Program 863 (No. 2015AA021001) and One Hundred Person Project (2015-43-D) of the Chinese Academy of Sciences.

References

[1] W.H. Organization, Water Quality and Health Strategy 2013–2020, World Health Organization, Geneva, Switzerland, 2013.
[2] M.M. Pendergast, E.M. Hoek, A review of water treatment membrane nanotechnologies, Energy Environ. Sci. 4 (2011) 1946–1971.
[3] M. Pasta, C.D. Wessells, Y. Cui, F. La Mantia, A desalination battery, Nano Lett. 12 (2012) 839–843.
[4] M. Elimelech, W.A. Phillip, The future of seawater desalination: energy, technology, and the environment, Science 333 (2011) 712–717.

[5] M. Sadrzadeh, T. Mohammadi, Sea water desalination using electrodialysis, Desalination 221 (2008) 440–447.
[6] K.Y. Wang, T.-S. Chung, M. Gryta, Hydrophobic PVDF hollow fiber membranes with narrow pore size distribution and ultra-thin skin for the fresh water production through membrane distillation, Chem. Eng. Sci. 63 (2008) 2587–2594.
[7] A. Al-Karaghouli, L.L. Kazmerski, Energy consumption and water production cost of conventional and renewable-energy-powered desalination processes, Renew. Sust. Energ. Rev. 24 (2013) 343–356.
[8] C.X. Jiang, Y.M. Wang, Z.H. Zhang, T.W. Xu, Electrodialysis of concentrated brine from RO plant to produce coarse salt and freshwater, J. Membr. Sci. 450 (2014) 323–330.
[9] T.W. Xu, C.H. Huang, Electrodialysis-based separation technologies: a critical review, AICHE J. 54 (2008) 3147–3159.
[10] C.J. Vörösmarty, P. McIntyre, M.O. Gessner, D. Dudgeon, A. Prusevich, P. Green, S. Glidden, S.E. Bunn, C.A. Sullivan, C.R. Liermann, Global threats to human water security and river biodiversity, Nature 467 (2010) 555–561.
[11] P. Malek, J. Ortiz, H. Schulte-Herbrüggen, Decentralized desalination of brackish water using an electrodialysis system directly powered by wind energy, Desalination 377 (2016) 54–64.
[12] A. El-Sebaii, E. El-Bialy, Advanced designs of solar desalination systems: a review, Renew. Sust. Energ. Rev. 49 (2015) 1198–1212.
[13] B.E. Logan, M. Elimelech, Membrane-based processes for sustainable power generation using water, Nature 488 (2012) 313–319.
[14] J.W. Post, H.V.M. Hamelers, C.J.N. Buisman, Energy recovery from controlled mixing salt and fresh water with a reverse electrodialysis system, Environ. Sci. Technol. 42 (2008) 5785–5790.
[15] R.E. Lacey, Energy by reverse electrodialysis, Ocean Eng. 7 (1980) 1–47.
[16] R. Pattle, Production of Electric Power by Mixing Fresh and Salt Water in the Hydroelectric Pile, 1954.
[17] E. Guler, Y.L. Zhang, M. Saakes, K. Nijmeijer, Tailor-made anion-exchange membranes for salinity gradient power generation using reverse electrodialysis, ChemSusChem 5 (2012) 2262–2270.
[18] M. Turek, B. Bandura, Renewable energy by reverse electrodialysis, Desalination 205 (2007) 67–74.
[19] J.G. Hong, B.P. Zhang, S. Glabman, N. Uzal, X.M. Dou, H.G. Zhang, X.Z. Wei, Y.S. Chen, Potential ion exchange membranes and system performance in reverse electrodialysis for power generation: a review, J. Membr. Sci. 486 (2015) 71–88.
[20] P. Długołęcki, J. Dąbrowska, K. Nijmeijer, M. Wessling, Ion conductive spacers for increased power generation in reverse electrodialysis, J. Membr. Sci. 347 (2010) 101–107.
[21] Q. Chen, Y.-Y. Liu, C. Xue, Y.-L. Yang, W.-M. Zhang, Energy self-sufficient desalination stack as a potential fresh water supply on small islands, Desalination 359 (2015) 52–58.
[22] R.A. Tufa, E. Curcio, E. Brauns, W. van Baak, E. Fontananova, G. Di Profio, Membrane distillation and reverse electrodialysis for near-zero liquid discharge and low energy seawater desalination, J. Membr. Sci. 496 (2015) 325–333.
[23] W. Li, W.B. Krantz, E.R. Cornelissen, J.W. Post, A.R. Verliefde, C.Y. Tang, A novel hybrid process of reverse electrodialysis and reverse osmosis for low energy seawater desalination and brine management, Appl. Energy 104 (2013) 592–602.
[24] Y. Jande, W. Kim, Integrating reverse electrodialysis with constant current operating capacitive deionization, J. Environ. Manag. 146 (2014) 463–469.
[25] P. Długołęcki, K. Nymeijer, S. Metz, M. Wessling, Current status of ion exchange membranes for power generation from salinity gradients, J. Membr. Sci. 319 (2008) 214–222.
[26] J.N. Weinstein, F.B. Leitz, Electric power from differences in salinity: the dialytic battery, Science 191 (1976) 557–559.
[27] I. Rubinstein, J. Pretz, E. Staude, Open circuit voltage in a reverse electrodialysis cell, Phys. Chem. Chem. Phys. 3 (2001) 1666–1667.
[28] E. Güler, Anion Exchange Membrane Design for Reverse Electrodialysis, Universiteit Twente, 2014.
[29] J. Veerman, M. Saakes, S.J. Metz, G.J. Harmsen, Reverse electrodialysis: performance of a stack with 50 cells on the mixing of sea and river water, J. Membr. Sci. 327 (2009) 136–144.
[30] S. Pawlowski, P. Sistat, J.G. Crespo, S. Velizarov, Mass transfer in reverse electrodialysis: flow entrance effects and diffusion boundary layer thickness, J. Membr. Sci. 471 (2014) 72–83.
[31] D.A. Vermaas, M. Saakes, K. Nijmeijer, Enhanced mixing in the diffusive boundary layer for energy generation in reverse electrodialysis, J. Membr. Sci. 453 (2014) 312–319.
[32] J. Veerman, M. Saakes, S.J. Metz, G.J. Harmsen, Reverse electrodialysis: a validated process model for design and optimization, Chem. Eng. J. 166 (2011) 256–268.
[33] M. Tedesco, E. Brauns, A. Cipollina, G. Micale, P. Modica, G. Russo, J. Helsen, Reverse electrodialysis with saline waters and concentrated brines: a laboratory investigation towards technology scale-up, J. Membr. Sci. 492 (2015) 9–20.
[34] A. Daniilidis, D.A. Vermaas, R. Herber, K. Nijmeijer, Experimentally obtainable energy from mixing river water, seawater or brines with reverse electrodialysis, Renew. Energy 64 (2014) 123–131.